

## Multi-Objective Tradeoff Studies of Directivity Achievable by Electrically Small Nanoloops

Jogender Nagar<sup>\*(1)</sup>, Sawyer D. Campbell<sup>(1)</sup>, Pingjuan L. Werner<sup>(1)</sup> and Douglas H. Werner<sup>(1)</sup>

(1) Electrical Engineering Department, The Pennsylvania State University, University Park, PA 16802 (USA)

### Abstract

Electrically small antennas typically suffer from a low radiation resistance, efficiency and bandwidth. In particular, achieving a high directivity (often called superdirectivity) from these structures is especially challenging, often requiring arrays which are extremely sensitive to mechanical and electrical tolerancing. Nonetheless, it was recently discovered that superdirectivity could be achieved by an electrically small gold nanoloop. Unfortunately, the initial design suffered from poor efficiency. A thicker nanoloop exhibits higher efficiency at the expense of a shift in the frequency range of high directivity to a region where the loop is no longer electrically small. This paper will explicitly show the tradeoffs between size, directivity and gain for nanoloops through a series of multi-objective optimizations.

### 1. Introduction

Over the past century, there has been an increasing desire to miniaturize antennas while maintaining high performance, particularly for wireless communications applications [1]. A seminal work by Wheeler [2] defines an electrically small antenna (ESA) as one that fits within a volume smaller than a sphere defined by  $k_b = \frac{2\pi b}{\lambda} < 1$  where  $b$  is the radius of the sphere and  $\lambda$  is the wavelength of operation. The paper describes the limitations of ESAs, including a low radiation resistance, increased loss and extremely narrow bandwidths. Wireless communications often requires antennas that are extremely directive, which has led to increasing interest in superdirectivity [1]. This concept can qualitatively be described as a significant enhancement in the directionality of the radiation of an antenna relative to a Hertzian or ideal dipole. The most well-known superdirective structures are arrays of antennas, each of which is fed with a particular amplitude and phase [1]. Unfortunately, these designs suffer from extreme sensitivity to mechanical and electrical tolerances. These problems are further exacerbated when attempting to design an electrically small array. The increased interest in both electrically small and superdirective antennas are unfortunately at odds with each other. In particular, Chu [3] theoretically explored the difficulties in achieving high directivity over a broad bandwidth for small antennas and provided an equation for the superdirective limit. According to these equations, the limit for superdirectivity approaches a value of zero as  $k_b$  approaches zero. A more suitable definition of superdirectivity in the context of electrically small antennas was derived by Geyi [4], in which the superdirective limit approaches the directivity of

a Huygen's source as  $k_b$  approaches zero. In a theoretical paper which derived the radiation properties of nanoloops it was discovered that an electrically small gold nanoloop could achieve superdirectivity [5]. This discovery was enabled by the fully analytical expressions derived in the paper, which allowed for extremely rapid parametric studies that would take excessive amounts of time when using full-wave simulations. While the ESA was superdirective, it suffered from a low efficiency. An increase in efficiency could be achieved by increasing the wire radius of the nanoloop, but this resulted in a shift in the frequency range of high directivity to a region of larger  $k_b$ . The discovery of types of tradeoffs is the goal of a multi-objective optimizer (MOO) [6]. This paper will employ the auto-adaptive MO genetic algorithm BORG [7] to study the tradeoffs between size, directivity and gain for nanoloops with a particular emphasis on attempting to achieve superdirectivity.

### 2. Radiation properties of nanoloops

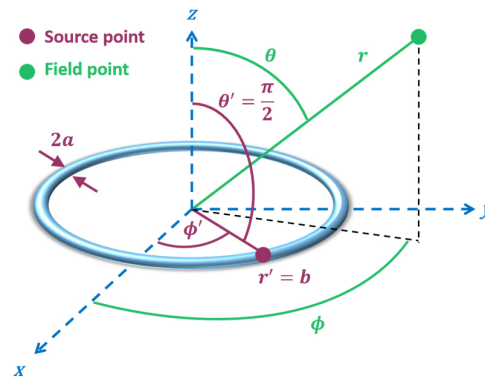


**Figure 1.** Geometry of the thin-wire nanoloop.

A full derivation of the radiation properties of thin-wire nanoloops was presented in [5]. The relevant results will be summarized here. Consider the nanoloop geometry of Figure 1 where the overall loop radius is given by  $b$  and the wire radius is represented by  $a$ . When using a thin-wire approximation, the surface current on the loop at the source points ( $r' = b, \phi', \theta' = \frac{\pi}{2}$ ) can be represented as a summation of standing wave modes:

$$I(\phi') = V_0 \left[ Y_0' + \sum_{m=1}^{\infty} Y_m' \cos(m\phi') \right] \quad (1)$$

where  $\mathbf{V}_0$  is the voltage source excitation located (without loss of generality) at  $\boldsymbol{\phi}' = \mathbf{0}$  and the modal admittances are given by:

$$\begin{aligned} Y'_0 &= [j\pi\eta_0 a_0 + (b/a)Z_s]^{-1} \\ Y'_m &= [j\pi\eta_0 (a_m/2) + (b/a)(Z_s/2)]^{-1} \end{aligned} \quad (2)$$

In these expressions  $\eta_0$  is the impedance of free space,  $a_m$  are coefficients given explicitly in [5] and  $Z_s$  is the surface impedance which takes into account the lossy dispersive nature of metals in the optical regime. Once the source currents are known, the near-zone electric fields at the field point  $(r, \theta, \phi)$  can be computed. In the far-zone the electric fields only depend on  $\theta$  and  $\phi$  and from these quantities the directivity in a given direction can be derived. A particular case of interest for this paper is the end-fire direction  $(\theta, \phi) = (90^\circ, 180^\circ)$  such that the directivity is represented by:

$$\begin{aligned} D(90^\circ, 180^\circ) &= \frac{2 \sum_{m=0}^{\infty} \sum_{n=0}^{\infty} [(-1)^m j^{m+n} Y'_m Y'_n J'_m(k_b) J'_n(k_b)]}{\sum_{m=0}^{\infty} |Y'_m|^2 \left[ \frac{1}{2} Q_{m-1, m-1}^{(1)}(k_b) + \frac{1}{2} Q_{m+1, m+1}^{(1)}(k_b) - \frac{m^2}{k_b^2} Q_{mm}^{(1)}(k_b) \right]} \end{aligned} \quad (3)$$

where  $J'_m$  are derivatives of the Bessel function of order  $m$  and  $Q_{mm}^{(1)}$  are the Q-type integrals defined explicitly in [5]. The radiation efficiency  $\epsilon$  depends on the material of the nanoloop and can be analytically derived using equations in [5]. Finally, the gain of the antenna is given by  $G = \epsilon D$ .

### 3. Multi-objective optimization

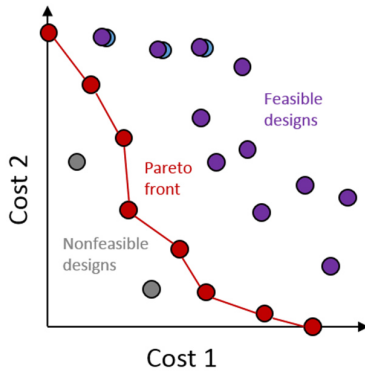


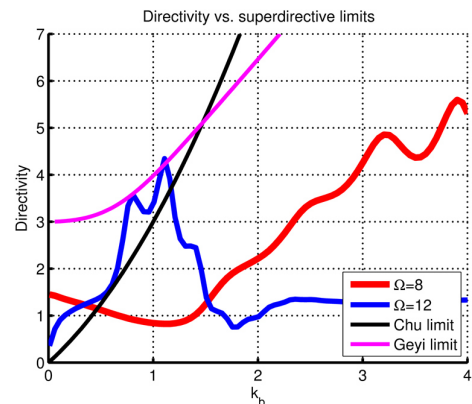
**Figure 2.** Example Pareto front.

Multi-objective optimizers (MOOs) allow the designer to explicitly view the trade-offs between multiple conflicting objectives by providing a set of solutions called the Pareto set in design parameter space and the Pareto front in objective space [6]. An example Pareto front is shown in Fig. 2. The ultimate goal is to simultaneously minimize both cost functions, but often that goal is not feasible within the design space. Instead, the goal of a MOO is to efficiently find the Pareto front. Every solution in this set is non-dominated, which means that improving one objective leads to degradation of at least one other objective. In addition, any solution which is better than a

solution on the Pareto front must not be feasible within the constraints of the optimization. BORG [7] is a genetic algorithm with multiple recombination and mutation operators which assimilates many of the features of MOOs developed during the past few decades. The algorithm automatically adjusts which recombination and mutation operators are used depending on their success rate. In addition, various parameters such as the population size are automatically adapted during the optimization process, leading to an algorithm which is extremely efficient while requiring very little tweaking of optimization parameters on the part of the user. While BORG is extremely efficient, MOOs tend to require more function evaluations to converge when compared to single-objective optimizers. Thankfully, the analytical results of Section 2 allow for extremely fast function evaluations, enabling a large number of multi-objective studies to be performed efficiently.

### 4. Results

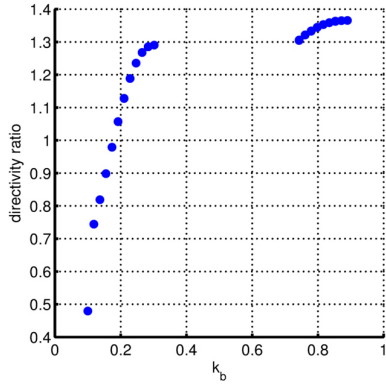
Using the expressions provided in Section 2, the directivity and gain of two gold nanoloops of circumference 600 nm and 3000 nm are shown in Figure 3, along with the superdirective limits as derived by Chu and Geyi. The directivity shown in red is for a nanoloop with thickness factor  $\Omega = 2 \ln\left(\frac{2\pi b}{a}\right) = 12$  while the result shown in blue is for a nanoloop with  $\Omega = 8$ . As can be seen, the thin loop has a directivity which exceeds both the Chu and Geyi limit. While the thicker loop exhibits a larger peak directivity, it does not exceed either limit. The efficiency of the thin loop is under 10% while the thicker loop achieves efficiencies which exceed 95% over the region of high directivity. Unfortunately, this region is shifted to higher frequencies where the loop is no longer electrically small. This implies a tradeoff between size, directivity and gain, which makes the analysis of this problem well-suited for multi-objective optimization.



**Figure 3.** Comparison of the directivity of gold nanoloops with the superdirectivity limits.

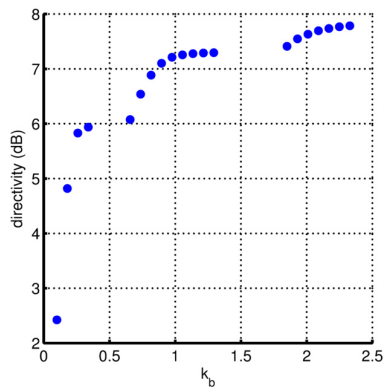
To further quantify this effect, a MOO was performed with the goals of maximizing the directivity ratio defined by the directivity of the nanoloop over the Geyi limit while

simultaneously minimizing the electrical size  $k_b$ . The resulting Pareto front is shown in Fig. 4. The Geyi superdirectivity limit cannot be surpassed until about  $k_b = 0.2$ . For the gold nanoloop considered in this problem, the maximum directivity ratio achievable is around 1.37.



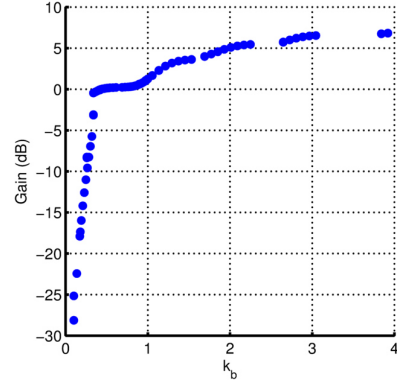
**Figure 4.** Pareto front for a gold nanoloop where the two objectives are maximizing the directivity ratio and minimizing  $k_b$ .

Figure 5 shows the Pareto front of a MOO where the two objectives are simultaneously maximizing the directivity and minimizing  $k_b$  for a gold nanoloop. As can be seen, directivities of up to 6 dB can be achieved for electrically small nanoloops with size  $k_b < 0.5$ . Interestingly, above  $k_b = 2.5$  the maximum directivity achievable actually decreases. However, this study did not consider efficiency. Further analysis shows that the loops below  $k_b = 0.5$  exhibit low efficiencies and the loops above this value tend to exhibit higher efficiencies.



**Figure 5.** Pareto front for a gold nanoloop where the two objectives are maximizing directivity and minimizing  $k_b$ .

To further quantify the effect of efficiency, a second MOO was performing with the objectives of maximizing gain while minimizing  $k_b$ . The resulting Pareto front is shown in Fig. 6. As can be seen, for low  $k_b$  the gain is below 0 dB. At around  $k_b = 0.8$ , the gain exceeds 0 dB and the maximum gain achievable increases monotonically as  $k_b$  increases.



**Figure 6.** Pareto front for a gold nanoloop where the two objectives are maximizing gain and minimizing  $k_b$ .

Finally, a MOO with all three objectives (directivity, gain and  $k_b$ ) was performed. The resulting Pareto front is shown in Fig. 7, where the y-axis is the gain in dB and the color is the directivity in dB. The results clearly show two branches for ESAs, one where the gain is high and the directivity is low and the other where the directivity is high and the gain is low. After around  $k_b = 1.5$ , high directivity and gain can be achieved simultaneously.

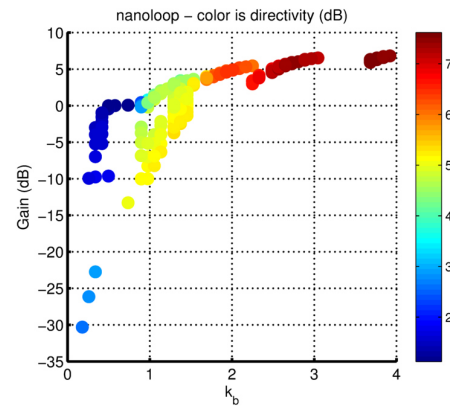


**Figure 7.** Comparison of the directivity of gold nanoloops with the superdirectivity limits.

## 5. Conclusion

A series of multi-objective optimizations showcased the tradeoffs between directivity, gain and electrical size for gold nanoloops. Further studies will consider the impact of using different materials and loading the loop with dielectric sections. In addition, the directivity and gain of nanoloop arrays will be investigated.

## 6. References

1. R. C. Hansen, *Electrically Small, Superdirective and Superconducting Antennas*, New York, USA: John Wiley and Sons, 2006.
2. H. A. Wheeler, "Fundamental limitations of small antennas," *Proceedings of the IRE*, **35**, 12, 1947, pp. 1479-4784, doi: 10.1109/JRPROC.1947.226199.
3. W. Geyi, "Physical limitations of antenna," *IEEE Trans. Antennas Propag.*, **51**, 8, 2003, pp. 2116-2123, doi: 10.1109/TAP.2003.814754.
4. L. J. Chu, "Physical limitations of omni-directional antennas," *J. Appl. Phys.*, **19**, 12, 1948, pp. 1163-1175, doi: 10.1063/1.1715038.
5. B. Q. Lu, J. Nagar, T. Yue, M. F. Pantoja and D. H. Werner, "Closed-form expressions for the radiation properties of nanoloops in the terahertz, infrared and optical regimes," *IEEE Trans. Antennas Propag.*, **65**, 1, 2017, pp. 121-133, doi: 10.1109/TAP.2016.2624150.
6. K. Deb, *Multi-Objective Optimization Using Evolutionary Algorithms*, Chichester, UK: John Wiley and Sons, 2001.
7. D. Hadka and P. Reed, "Borg: an auto-adaptive many-objective evolutionary computing framework," *Evolutionary Computation*, **21**, 2, 2013, pp. 231-259, doi:10.1162/EVCO.a.00075.